

Centralised and Distributed Optimization for Aggregated Flexibility Services Provision

Pol Olivella-Rosell¹, Student Member, IEEE, Francesc Rullan, Student Member, IEEE, Pau Lloret-Gallego², Eduardo Prieto-Araujo³, Member, IEEE, Ricard Ferrer-San-José, Student Member, IEEE, Sara Barja-Martinez, Sigurd Bjarghov, Student Member, IEEE, Venkatachalam Lakshmanan, Ari Hentunen⁴, Member, IEEE, Juha Forsström, Stig Ødegaard Ottesen⁵, Roberto Villafafila-Robles⁶, Member, IEEE, and Andreas Sumper⁷, Senior Member, IEEE

Abstract—The recent deployment of distributed battery units in prosumer premises offer new opportunities for providing aggregated flexibility services to both distribution system operators and balance responsible parties. The optimization problem presented in this paper is formulated with an objective of cost minimization which includes energy and battery degradation cost to provide flexibility services. A decomposed solution approach with the alternating direction method of multipliers (ADMM) is used instead of commonly adopted centralised optimization to reduce the computational burden and time, and then reduce scalability limitations. In this work we apply a modified version of ADMM that includes two new features with respect to the original algorithm: first, the primal variables are updated concurrently, which reduces significantly the computational cost when we have a large number of involved prosumers; second, it includes a regularization term named Proximal Jacobian (PJ) that ensures the stability of the solution. A case study is presented for optimal battery operation of 100 prosumer sites with real-life data. The proposed method finds a solution which is equivalent to the centralised optimization problem and is computed between 5 and 12 times faster. Thus, aggregators or large-scale energy communities can use this scalable algorithm to provide flexibility services.

Index Terms—Flexibility, smart grid, distributed optimization.

Manuscript received July 1, 2019; revised October 10, 2019 and December 18, 2019; accepted December 18, 2019. Date of publication February 3, 2020; date of current version June 19, 2020. This work was supported in part by the European Union's Horizon 2020 Research and Innovation Program through INVADE H2020 Project (2017–2019) under Grant 731148, in part by the Ministerio de Ciencia, Innovación y Universidades under Project RTI2018-099540, and in part by InnoEnergy Ph.D. School. Paper no. TSG-00926-2019. (Corresponding author: Pol Olivella-Rosell.)

Pol Olivella-Rosell, Pau Lloret-Gallego, Eduardo Prieto-Araujo, Ricard Ferrer-San-José, Sara Barja-Martinez, Roberto Villafafila-Robles, and Andreas Sumper are with CITCEA, Universitat Politècnica de Catalunya, 08036 Barcelona, Spain (e-mail: pol.olivella@outlook.com).

Francesc Rullan is with the Department of Computer Science, University College London, London WC1E 6BT, U.K.

Sigurd Bjarghov and Venkatachalam Lakshmanan are with the Department of Electric Power Engineering, NTNU, 7491 Trondheim, Norway.

Ari Hentunen and Juha Forsström are with the VTT Technical Research Centre of Finland Ltd., 02150 Espoo, Finland.

Stig Ødegaard Ottesen is with eSmart Systems AS, 1783 Halden, Norway. Color versions of one or more of the figures in this article are available online at <http://ieeexplore.ieee.org>.

Digital Object Identifier 10.1109/TSG.2019.2962269

NOMENCLATURE

Abbreviations

ADMM	Alternating direction method of multipliers
ALFM	Aggregated level flexibility management
ALFO	Aggregated level flexibility offer
BRP	Balance responsible party
DSO	Distribution system operator
EU	European Union
FD	Flexibility device
FR	Flexibility request
HEMS	Home energy management system
LFM	Local flexibility market
P2P	peer-to-peer
PJ	Proximal Jacobian
PTU	Programing time unit
PV	Photovoltaic
SOC	State-of-charge.

Indices and Sets

\mathcal{I}	Set of prosumer sites, indexed by i
\mathcal{J}	Set of segments for battery SOC, indexed by j
\mathcal{T}	Set of periods/time slots in the planning horizon, indexed by t
\mathcal{T}^{\pm}	Subset of periods with up (+) or down (−) regulation.

Parameters

$A_i^{bat, ch}$	Battery charging efficiency in site i [p.u.]
$A_i^{bat, dis}$	Battery discharging efficiency in site i [p.u.]
$C_{i,j}$	Marginal battery cycling ageing cost per segment j in site i [EUR/kWh]
FR_t	Flexibility request from BRP/DSO in period t [kWh]
O_i^{max}	Maximum battery SOC in site i [kWh]
O_i^{min}	Minimum battery SOC in site i [kWh]
$O_{i,j}^{max}$	Maximum battery SOC in segment j in site i [kWh]
$P_{i,t}^{buy}$	Price at energy part for buying electricity in period t in site i [EUR/kWh]

$P_{i,t}^{gen}$	Penalty cost for curtailing photovoltaic energy production [EUR/kWh] of site i in period t	$\sigma_{i,t,j}^{seg,soc}$	Amount of electricity stored in the battery segment j in time step t in site i [kWh]
$P_{i,t}^{sell}$	Price at energy part for buying electricity in period t in site i [EUR/kWh]	$\sigma_{i,t}^{ch}$	Battery charging energy in time step t in site i [kWh]
Q_i^{ch}	Maximum battery charging energy per time unit in site i [kWh]	$\sigma_{i,t}^{dis}$	Battery discharging energy in time step t in site i [kWh]
Q_i^{dis}	Maximum battery discharging energy per time unit in site i [kWh]	$\sigma_{i,t}^{soc}$	Battery SOC in time step t in site i [kWh]
S_i^{LT}	Amount of time intervals in battery lifetime in site i [years]	$\sigma_{i,t}^{ch}$	Amount of electricity charged to the battery unit in period t in site i [kWh]
W_i^{bat}	Battery voltage charging tuning factor in site i	$\sigma_{i,t}^{dis}$	Amount of electricity discharged from the battery unit in period t in site i [kWh]
$W_{i,t}^l$	Inflexible load consumption in period t in site i [kWh]	$\sigma_{i,t}^{soc}$	Battery SOC of site i in time step t at the end of period t [kWh]
W_t^{base}	Aggregated baseline consumption in period t [kWh]	$\zeta_{i,t}^{flex}$	Total cost for activating flexibility in period t in site i [EUR]
W_t^{flex}	Aggregated electricity consumption in period t after meeting the flexibility request [kWh]	$a^{inv,ch}(\cdot)$	Battery inverter charging efficiency function [p.u.]
X_i^{exp}	Maximum electricity export capacity of site i per period [kWh]	$a^{inv,dis}(\cdot)$	Battery inverter discharging efficiency function [p.u.].
X_i^{imp}	Maximum electricity import capacity of site i per period [kWh].		

Parameters ADMM

ϵ^{dual}	Dual error threshold
ϵ^{pri}	Primal error threshold
γ	Damping parameter
$\lambda_t^{(k)}$	Dual variable for constrained period t in iteration k
$\rho^{(k)}$	Penalty parameter in iteration k
τ^{decr}	Decremental parameter to decelerate penalty parameter ρ
τ^{incr}	Incremental parameter to accelerate penalty parameter ρ
CT^{max}	Maximum computation time threshold
K^d	Penalty for the dual error
K^i	Penalty for accumulated primal error
$r_t^{(k)}$	Primal error for constrained period t in iteration k [kWh]
$s_t^{(k)}$	Dual error for constrained period t in iteration k [kWh].

Variables

$\chi_{i,t}^{buy}$	Amount of electricity bought in period t by site i [kWh]
$\chi_{i,t}^{sell}$	Amount of electricity sold in period t by site i [kWh]
$\delta_{i,t}^{bat}$	Binary variable=1 if battery of site i is charged in period t , else 0
$\delta_{i,t}^{buy}$	Binary variable=1 if site i is importing electricity in period t , else 0
$\delta_{i,t}^{sell}$	Binary variable=1 if site i is exporting electricity in period t , else 0
$\psi_{i,t}$	Amount of electricity produced from generating unit in period t in site i [kWh]
$\sigma_{i,t,j}^{seg,ch}$	Battery charging energy in time step t in segment j in site i [kWh]
$\sigma_{i,t,j}^{seg,dis}$	Battery discharging energy in time step t in segment j in site i [kWh]

I. INTRODUCTION

IN THE context of smart grids and flexibility services in place, balance responsible parties (BRPs) and distribution system operators (DSOs) can benefit by activating flexibility in distribution grids. Electricity price volatility in Europe is increasing in electricity markets during scarcity periods, for example due to fluctuating generation. Additionally, distributed generation could compromise the stable operation of distribution grids and cause congestions.

In this scenario, remotely controlled distributed batteries at prosumer premises could help to provide flexibility services for dealing with the issues mentioned above, like INVADE H2020 project proposes [1]. An energy cloud platform can remotely manage batteries and it can be operated by an aggregator with a portfolio formed by a group of prosumer sites. These sites can belong to different BRPs and DSO, and they can be grouped according to their grid and BRP zones. For instance, all sites with contracts of flexibility provision for DSO service within the same grid zone can be operated to respond to a DSO flexibility request (FR). A grid zone is a group of end-users defined by the DSO according to its confidential information such as grid configuration and potential congestions. Therefore, DSOs can increase their grid capacity to host more renewable generation or reduce network congestions during peak production or consumption periods respectively. Similarly, during the periods of high prices, BRPs could maintain their day-ahead generation and consumption portfolio by activating flexibility instead of paying penalties for their deviations or paying high intraday market costs to keep their energy portfolio [2]. The present paper deals with the short-term operation of distributed batteries behind-the-meter in order to provide flexibility services to BRPs or DSOs at the minimum cost.

A. Home Energy Management Systems

Previous work in topics of decision-making at site level and home energy management systems (HEMS) include

optimization algorithms to find the best possible scheduling of flexibility devices (FDs). Therefore, HEMS algorithms consider that sites are independent of each other, metered separately and focuses on individual site's benefit. A detailed analysis of HEMS and FD is presented in [3], [4], which present different types of optimization problem formulations to achieve similar objective functions. Profitability and operation possibilities of distributed generation, home batteries and electric vehicles depend on the electricity tariff structure for the point of connection. For instance, [5] presents different electricity markets and electricity tariff structures for HEMS. Reference [6] provides an economic analysis of storage for self-consumption in Germany and concludes that the cases with high demand and larger PV installations are the only profitable cases. However, aggregated flexibility services can provide additional value for storage owners and the present paper provides two optimization algorithms that combines both site and their aggregated level solution.

B. Aggregated Flexibility Services

Moreover, aggregated flexibility can be used not only for providing technical services to cope with distribution grid congestion issues [7] or to increase the grid hosting capacity [8], but also can help to improve the efficiency of electricity markets [9]. For instance, [10] presents a collection work that represents current trends in energy management systems from the aggregators point of view. In addition, [11] proposes a centralised method for aggregators to schedule flexibility in different electricity markets. Furthermore, [12] discusses the potential value that aggregators may provide under different regulatory frameworks and how the inadequacy in regulation can harm other power system objectives.

The most recent works include battery aggregated operation in distribution grids [13]–[22]. Reference [13] presents an analysis of operating central storage units directly connected to medium-voltage grids to provide power system services. Reference [14] compares the technical service provision to self-consumption maximization service using a centralised battery at distribution level. However, [13], [14] do not consider distributed batteries at prosumer level which can change their operation with an economic incentive mechanism. Furthermore, [15] formulates a HEMS capable of providing flexibility to DSOs and [16] presents a bi-level agent-based optimization algorithm including the DSO operation cost. Unfortunately, this algorithm cannot be implemented in some countries. For instance, the European Union (EU) electricity market unbundling does not allow to merge DSO and end-users objectives as grid information cannot be shared with aggregators. Thus, current studies for European Union applications assume DSO quantifies the flexibility needed to solve the grid problem in accordance to their operating costs as a separate problem and the aggregator assists the DSO by grid zones as suggested in [17] and [18]. Reference [19] presents a flexibility provision HEMS and it is solved with an heuristic particle swarm optimization algorithm. Though, augmented Lagrangian methods facilitate to find optimal solutions in a reasonable computational time in a distributed manner.

Finally, [20] presents a market based flexibility exchange framework for multiple aggregators competing to solve the same congestion problem. It provides basis to formulate algorithms that are capable to deal with multiple aggregators and the work presented in this paper answers the question regarding re-scheduling FDs where an aggregator needs to compromise by activating a certain flexibility volume. The case of multiple aggregators competing for the same service is out of the scope of this paper.

Another way of handling large-scale flexibility portfolios is using aggregation and disaggregation techniques like [21], [22]. Reference [21] presents a scalable aggregation decision-making algorithm for scheduling electric vehicles. Reference [22] presents a scalable approach for flexible energy systems based on zonotopic sets. Instead of using aggregation and disaggregation steps for decision-making, this work has the advantage of using simple formulation of site-level cost functions and constraints while managing sensitive information independently.

C. Alternating Direction Method of Multipliers

The alternating direction method of multipliers (ADMM) is a decomposition algorithm for distributed convex optimization, but it can be also considered as an heuristic algorithm for solving non-convex problems [23]. Nowadays, ADMM is widely applied in distributed computing environments for power systems. ADMM can be used to solve problems involving large amount of data and variables in the field of smart grids. For example, a fully distributed optimal power flow problem is presented in [24], and [25] suggests an ADMM approach for a generation investment problem in electricity markets. Reference [26] presents a distributed dispatching ADMM-based algorithm for coordinating PV inverters and conventional voltage regulation devices in distribution networks. Regarding load restoration strategies, [27] shows an algorithm for unbalanced distribution systems considering distributed energy resources local control and [28] presented a coordination algorithm to restore transmission and distribution systems, both based on ADMM. In the field of ancillary services and real time prices, [29] shows a decentralised multi-block ADMM for primary frequency control and [30] proposes a distributed consensus-based ADMM algorithm to activate demand response considering communication uncertainties.

Cloud computing services and big data research can also benefit from ADMM algorithms as they allow to distribute computational power to solve different sub-problems that can be assigned to different processing units [23]. Reference [31] presents the mathematical formulation of network energy management, robust state estimation and security constrained optimal power flow problems in a distributed manner via ADMM. Reference [32] formulates the parallel multi-block ADMM for generic problems like exchange problem, ℓ_1 -minimization and distributed large-scale ℓ_1 -minimization, and tested them on a cloud computing platform.

For applications regarding energy management in smart grids, [33] reviews the work of different authors on community-based and peer-to-peer (P2P) market mechanisms.

Reference [34] solves a novel cost allocation in P2P electricity markets using the consensus ADMM algorithm. Reference [35] formulates a distributed operation of energy collectives using an ADMM algorithm by varying penalty parameter adapted to each case study. Reference [36] presents a distributed optimization for community microgrids where each site has its own HEMS. However, the applied ADMM method is very case-sensitive to the augmented Lagrangian penalty parameter for meeting the energy balance constraint. Therefore, this paper presents a novel two-steps accelerated method which uses the Proximal Jacobian regularization to find optimization solutions faster without large variations in the objective function.

D. Summary of Contributions

Under the before mentioned change of paradigm presented in the previous references about energy/flexibility exchanges at distribution level, the present paper aims to contribute in the area of large-scale aggregator portfolio optimal scheduling. The main contributions of this paper are threefold:

- Formulation of a centralised optimization problem for aggregated flexibility service provision from prosumers with batteries to third parties like DSOs and BRPs considering battery ageing factors. The framework of this problem includes an aggregator in charge of scheduling batteries for prosumer minimum cost operation under two situations: regular operation and constrained operation when BRP/DSO send a flexibility request to aggregator.
- Distributed version of the previous aggregation problem including the detailed battery ageing model using a novel accelerated ADMM algorithm to find suitable solutions in less than 10 minutes. This problem could be suitable for centralized aggregator as a decision maker or distributed decision frameworks like P2P. In both frameworks, batteries need to receive new control signals every 15 minutes to adapt to new conditions such as solar radiation or new flexibility requests.
- Sensitivity analysis of the centralised and distributed algorithms in relation to the aggregator portfolio size and the number of variables, ADMM algorithm acceleration parameters, and execution time.

The case study presented is the evidence for ease of implementation of the distributed algorithm.

II. FRAMEWORK DESCRIPTION

Aggregators can respond to flexibility requests from BRPs for day-ahead and intraday portfolio optimization or from DSOs to reduce network congestions [2]. A FR can be defined as the difference between the baseline and the desired load profile. It can be measured in energy per programming time unit (PTU). PTUs can vary depending on the applicant and the application case. For instance, BRPs dealing with electricity markets would be interested in hourly PTUs. However, DSOs could be interested in higher time granularity with quarterly PTUs or even 5 minutes time resolution. This paper goes for hourly PTUs for simplicity but the formulation is valid for different time steps. A FR can be for up-regulation which

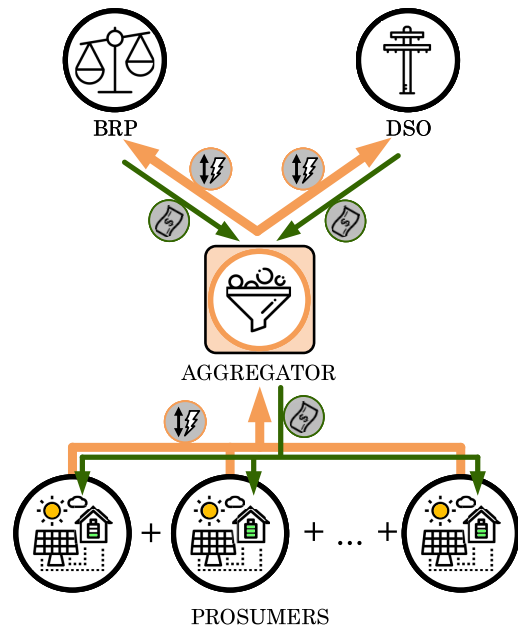


Fig. 1. Local flexibility market framework.

corresponds to an increase in generation or a decrease in consumption. Similarly, the FR for down-regulation can be defined as a decrease in generation or an increase in consumption. The baseline load profile at transmission level is defined based on market settlements, which cannot be applied at distribution grid level. Moreover, DSOs, BRPs and aggregators have different portfolios and their baselines cannot be analogous. In the present framework, DSOs and BRPs use aggregator's load baseline as reference for their flexibility settlements.

This paper applies the local flexibility market (LFM) framework presented in [37] where an aggregator is responsible for re-scheduling FDs to meet an external FR without violating the end-user agreements. Fig. 1 shows the framework and all involved agents related to flexibility exchanges. The aggregator is in charge of managing the energy cloud platform which remotely controls distributed devices, such as batteries, in prosumer premises. BRP-aggregator and DSO-aggregator are linked through flexibility contracts which specify the conditions for flexibility trading as explained in [37]. As mentioned above, BRP and DSO are interested in activating flexibility and they send FRs to aggregator. In this scenario, aggregator is in charge of seeking the cheapest combination of flexibility activations to reduce operational cost such as battery degradation. Thus, prosumers provide flexibility to BRP/DSO (orange arrows), who pay the aggregator for providing these services (green arrows). A portion of the flexibility exchange benefits can go to prosumers. All deviations from BRP's market position represent a money flow which is out of the scope of this work as the BRP is responsible of taking them into account before submitting FRs.

Nevertheless, aggregator agent could be surpassed and every prosumer could decide their own contribution to the FR individually without any third party. In such case, BRPs and DSOs could interact directly with prosumers and the distributed optimal flexibility provision algorithm presented in this work

could be applied. Additionally, this possibility would allow end-users to protect their personal information such as consumption patterns and habits. This possibility opens many aspects to be discussed in detail but this is not the objective of the present work and future publications could discuss it in more detail.

Additionally, aggregator applies a traffic light system as suggested in [18], [37] to solve potential conflicts between simultaneous or even contradictory FR. Decisions are made centrally using two-way communications, where aggregators send direct control signals and receive metered consumption and status from each FD. In [38] it is stated that the architecture used has potential scalability limitations. However, in this paper it is shown that distributed optimization can overcome scalability issues.

III. SITE LEVEL OPTIMIZATION PROBLEM

The site level optimization problem defined in (1) schedules all FDs by considering battery and PV constraints, forecasted inputs and costs for the site, but not the FR. Nomenclature is listed in the Appendix. This problem is formulated as a mixed-integer linear programming (MILP) as it follows. Linear objective function (1a) represents the cost minimization for prosumer site i including flexibility costs for either using the battery or curtailing the PV if needed. Purchasing ($P_{i,t}^{buy}$) and selling prices ($P_{i,t}^{sell}$) typically come from retailer contracts which are known in advance. Otherwise, prices can be indexed to day-ahead markets. The present framework assumes to be executed some hours in advance of the operation day, when the day-ahead prices are already published. (1b) is the electricity balance of site i which depends on the forecasted inflexible load ($W_{i,t}^l$) and PV generation ($\psi_{i,t}$). Additionally, (1c) and (1d) limit site import and export capacity and (1e) ensures site i does not import and export electricity simultaneously at period t . Thus, each prosumer site problem has 72 binary variables including the battery model. Battery charging ($\sigma_{i,t}^{ch}$) and discharging ($\sigma_{i,t}^{dis}$) decision variables from Eq. (1b) are limited by common Eq. (10), cycle ageing Eq. (11), calendar ageing Eq. (12), and voltage Eq. (13). Moreover, the battery system efficiency depends on the inverter power-efficiency relation and a constant battery efficiency. The battery model is explained in detail in the Appendix. Constraint (1f) considers the cost of activating flexibility from battery of each site i as the addition of cycling ageing ($\beta_{i,t}^{cyc}$) and calendar ageing costs ($\beta_{i,t}^{cal}$) from Eq. (12) and Eq. (11e) respectively. Battery flexibility cost depends on charging and discharging decisions [39].

The aggregated result of all prosumer site optimization problems is the load baseline in aggregated flexibility services.

$$\min_{\chi, \zeta} \sum_{i \in \mathcal{T}} \left(P_{i,t}^{buy} \chi_{i,t}^{buy} - P_{i,t}^{sell} \chi_{i,t}^{sell} + \zeta_{i,t}^{flex} \right) \quad \forall i \quad (1a)$$

$$\text{s.t. } \chi_{i,t}^{buy} + \sigma_{i,t}^{dis} + \psi_{i,t} = \chi_{i,t}^{sell} + \sigma_{i,t}^{ch} + W_{i,t}^l \quad \forall i, t \quad (1b)$$

$$\chi_{i,t}^{buy} \leq \delta_{i,t}^{buy} \chi_i^{imp} \quad \forall i, t \quad (1c)$$

$$\chi_{i,t}^{sell} \leq \delta_{i,t}^{sell} \chi_i^{exp} \quad \forall i, t \quad (1d)$$

Algorithm 1: Centralized Optimal Flexibility Provision

Input: $W_{i,t}^l, \psi_{i,t}$

- 1 Optimize each site flexibility according to Eq. (1) for minimum cost operation
- 2 Output: $\chi_{i,t}^{buy}, \chi_{i,t}^{sell}, \sigma_{i,t}^{ch}, \sigma_{i,t}^{dis}$
- 3 Send baseline energy notice ($W_t^{base} = \sum_i \chi_{i,t}^{buy} - \chi_{i,t}^{sell}$) to BRP/DSO
- 4 **if** $FR_t \neq 0$ **then**
- 5 Prioritize FR_t of each period
- 6 Optimize each site flexibility to minimize their costs and meeting the FR according to ALFO problem (2)
- 7 Output: $\chi_{i,t}^{buy}, \chi_{i,t}^{sell}, \sigma_{i,t}^{ch}, \sigma_{i,t}^{dis}$ and flexibility offer to BRP/DSO
- 8 **if** Accepted $FR_t \neq 0$ **then**
- 9 Optimize each site flexibility including the accepted FR according to ALFM problem (4)
- 10 Output: $\chi_{i,t}^{buy}, \chi_{i,t}^{sell}, \sigma_{i,t}^{ch}, \sigma_{i,t}^{dis}$ from Eq. (4) including accepted FR_t
- 11 Send control signals ($\sigma_{i,t}^{ch}, \sigma_{i,t}^{dis}$) from Eq. (4) to batteries.
- 12 **else**
- 13 Send control signals ($\sigma_{i,t}^{ch}, \sigma_{i,t}^{dis}$) from Eq. (1) to batteries.
- 14 **end**
- 15 **else**
- 16 Send control signals ($\sigma_{i,t}^{ch}, \sigma_{i,t}^{dis}$) from Eq. (1) to batteries.
- 17 **end**

$$\delta_{i,t}^{buy} + \delta_{i,t}^{sell} \leq 1 \quad \forall i, t \quad (1e)$$

$$\zeta_{i,t}^{flex} = \beta_{i,t}^{cyc} + \beta_{i,t}^{cal} \quad \forall i, t. \quad (1f)$$

IV. CENTRALISED FLEXIBILITY PROVISION

The centralised flexibility service provision algorithm formulated in this section is composed of two consecutive problems:

- Aggregated level flexibility offer (ALFO) formulation finds the available flexibility without violating local constraints according to the FR.
- Aggregated level flexibility management (ALFM) problem finds the cheapest scheduling of FDs once the aggregator received a FR acceptance from a BRP and/or DSO.

A. Centralised Flexibility Provision Algorithm

The centralised Algorithm 1 for aggregated flexibility scheduling first optimizes the battery of each prosumer to reduce energy cost individually following the problem (1) based on the forecasted values of electricity consumption and PV production. The obtained result is the energy baseline considering the optimal battery scheduling. This information is sent to the DSO and BRP. The DSO baseline energy notice is referred to the prosumers of each grid zone and BRP needs to know the consumption of its customers. Based on this information, DSO and BRP can send FRs if needed. Then, the aggregator executes the ALFO problem (2) to calculate the flexibility offer for the BRP/DSO based on the FR. As it could be higher than the portfolio capability, it is necessary to optimize FDs for offering equal or less flexibility

than the FR. Each DSO and BRP can decline, accept the offer fully or only parts of it. In case the offer is completely accepted, the aggregator can use flexibility scheduling from the ALFO optimization step to generate control signals. In case the flexibility offer is partially accepted, the aggregator has to execute the ALFM problem (4) in order to re-schedule FDs to meet the accepted FR. In contrast to the previous ALFO problem, aggregator already knows FR is reachable and ALFM optimization needs equal or more flexibility than the accepted FR as slightly more flexibility is not a real problem if it is cheaper than less flexibility. This is necessary in case of having binary decision variables as it can be difficult to exactly match the requested flexibility amount of a FR. The Algorithm 1 prevents infeasible instances due to this two-steps structure and two optimization problems.

This process schedules all FDs for an optimization planning horizon and it can be repeated periodically considering new forecasted inputs and FRs. It is to be noted that the baseline demand could be updated each time new forecasted values are obtained. However, it can be convenient to keep a constant baseline within a day to avoid confusions between aggregator, BRP and DSO about the reference scenario. Reference [40] presents example cases of aggregated flexibility services using this architecture.

B. ALFO Problem Formulation

Objective function (2a) considers the electricity and flexibility costs of each site i over the planning horizon. This problem is formulated as an mixed-integer nonlinear programming (MINLP) as flexibility costs include quadratic penalty for the flexibility that is not served. The penalty is defined as the difference between the total load scheduled in each site optimization problem ($\chi_{i,t}^{tot}$) as per constraint (3a), and the expected load after applying a FR as per constraint (3b). In case of a lack of flexibility where the aggregator cannot meet the FR completely, the quadratic penalty ensures that the flexibility provided will follow the shape of the FR. Otherwise, a linear penalty in the objective function would reduce the computational burden but not necessarily generate flexibility provision for all constrained time periods. From practical point of view, it means to consider all flexibility time periods with the same priority according to the flexibility power requested and the aim is to provide flexibility during all requested periods. As previously explained, constraints (2b) and (2c) ensure that the activated amount of flexibility is less or equal to the up and down FR respectively. Additionally, constraints (2d) and (2e) are necessary in cases of grid congestions to ensure that the rebound effect is not causing new load peaks before or after the activation of the FR.

$$\min_{\chi_i, \zeta_i} \sum_{i \in \mathcal{I}} \sum_{t \in \mathcal{T}} \left(P_{i,t}^{buy} \chi_{i,t}^{buy} - P_{i,t}^{sell} \chi_{i,t}^{sell} + \zeta_i^{flex} + P^{penal} \sum_{t \in \mathcal{T}^{\pm}} \left(W_t^{flex} - \sum_{i \in \mathcal{I}} \chi_{i,t}^{tot} \right)^2 \right) \quad (2a)$$

$$\text{s.t.} \quad \sum_{i \in \mathcal{I}} \chi_{i,t}^{tot} \geq W_t^{flex} \quad \forall t \in \mathcal{T}^+ \quad (2b)$$

$$\sum_{i \in \mathcal{I}} \chi_{i,t}^{tot} \leq W_t^{flex} \quad \forall t \in \mathcal{T}^- \quad (2c)$$

$$\sum_{i \in \mathcal{I}} \chi_{i,t}^{buy} \leq \max(W_t^{flex}) \quad \forall t \quad (2d)$$

$$\sum_{i \in \mathcal{I}} \chi_{i,t}^{sell} \leq \max(W_t^{flex}) \quad \forall t \quad (2e)$$

$$\chi_{i,t}^{tot} = \chi_{i,t}^{buy} - \chi_{i,t}^{sell} \quad (3a)$$

$$W_t^{flex} = W_t^{base} - FR_t. \quad (3b)$$

C. ALFM Problem Formulation

Once the aggregator estimates the available flexibility, it is communicated as flexibility offers to the BRP or DSO. If they accept the offer either partially or entirely, the aggregator can execute the ALFM optimization problem to fulfil it. The objective function (4a) is the same as objective function (2a) but removing the quadratic penalty for not meeting the FR as the ALFO problem ensures there is sufficient flexibility. In this MILP optimization problem, constraints (4b) and (4c) ensure enough flexibility and the site cost is penalizing the excessive battery usage. We can include constraints (2d) and (2e) if it is necessary to avoid new undesired load peaks like in Section IV-B.

$$\min_{\chi_i, \zeta_i} \sum_{i \in \mathcal{I}} \sum_{t \in \mathcal{T}} \left(P_{i,t}^{buy} \chi_{i,t}^{buy} - P_{i,t}^{sell} \chi_{i,t}^{sell} + \zeta_i^{flex} \right) \quad (4a)$$

$$\text{s.t.} \quad \sum_{i \in \mathcal{I}} \chi_{i,t}^{tot} \leq W_t^{flex} \quad \forall t \in \mathcal{T}^+ \quad (4b)$$

$$\sum_{i \in \mathcal{I}} \chi_{i,t}^{tot} \geq W_t^{flex} \quad \forall t \in \mathcal{T}^- \quad (4c)$$

The main advantage of this formulation is its simplicity. However, problems (2) and (4) may have scalability limitations as mentioned before. Therefore, this paper explores methods to decompose the problem to improve its computational performance with large-scale implementations.

V. DISTRIBUTED FLEXIBILITY PROVISION

The distributed flexibility provision algorithm aims to solve the same problem previously presented in Section IV but using the alternating direction method of multipliers (ADMM) in order not only to improve computational performance in terms of memory usage and execution time, but also to keep end-user private data separately. As stated before, this formulation could be extended for peer-to-peer flexibility exchange frameworks as the algorithm could be executed in distributed computation frameworks. The proposed distributed algorithm is based on the optimal exchange problem presented in [23] but applied in local flexibility markets where each prosumer settles their contribution to the FR in parallel. Therefore, high performance computers or energy cloud platforms can solve distributed algorithms with less scalability limitations using multi-processor architectures. Additionally, the distributed formulation can deal with FRs that surpasses the available flexibility. Thus, both ALFO and ALFM are substituted by a single distributed optimization algorithm.

A. Augmented Lagrangian

The augmented Lagrangian relaxation (\mathcal{L}_ρ) is presented in (5) and it is equivalent to the previous problems Eqs. (2) and (4) relaxing constraints (2b), (2c), (4b), (4c). It is to be noted that previous constraints are formulated as inequalities. However, they can be rewritten as equalities for simplicity as small errors above or below FR threshold are not significant from engineering point of view. Thus, Eq. (5) assumes constraint (2b) as equality because the ADMM is designed for equality constraints and final error is small enough for the case study. According to [23], the regular ADMM algorithm consists of an iterative process to minimize \mathcal{L}_ρ and to update the dual variable ($\lambda_t^{(k)}$) for each constrained period t by giving a fixed penalty parameter ($\rho > 0$). In ADMM implementations, it is necessary to identify generic values for penalty parameters (ρ) capable of providing satisfying solutions in reasonable computation time for multiple cases.

$$\begin{aligned} \mathcal{L}_\rho = & f(x_i) + \sum_{t \in \mathcal{T}^\pm} \lambda_t^{(k)} \left(\chi_{i,t}^{tot} - \frac{W_t^{flex}}{N} \right) \\ & + \frac{\rho}{2} \sum_{t \in \mathcal{T}^\pm} \left\| \chi_{i,t}^{tot} + \sum_{\substack{j \in \mathcal{I} \\ j \neq i}} \chi_{j,t}^{tot,(k)} - \left(W_t^{flex} \right) \right\|^2 \end{aligned} \quad (5)$$

In the present work, each site i can decide individually their contribution to the FR according to its cost function (6a) using (x_i) as decision variable vector (6b), the dual variable ($\lambda_t^{(k)}$) and the result of other sites ($j \in \mathcal{I}, j \neq i$) in the previous step (k). It is noticeable x_i contains continuous variables $\chi_{i,t}^{tot}$ and $\psi_{i,t}^{flex}$ from problem (1). Therefore, ADMM only contains continuous variables. Additionally, every step branch-and-bound solves the site problem including binary variables and constraints (1). Therefore, Eq. (5) can be solved with MILP solvers such as Gurobi once $\lambda_t^{(k)}$ is updated.

$$f(x_i) = \sum_{t \in \mathcal{T}} \left(p_{i,t}^{buy} \chi_{i,t}^{buy} - p_{i,t}^{sell} \chi_{i,t}^{sell} + \zeta_{i,t}^{flex} \right) \quad (6a)$$

$$x_i = \left[\chi_{i,t}^{tot}, \zeta_{i,t}^{flex} \right] \quad (6b)$$

Finally, it is important to highlight Problems (1), (2), (4) and (5) are MILP, so non-convex. Therefore, ADMM nor other decomposition techniques ensure to find the global optimum solution. However, Section VI shows the present work is able to converge and find a sub-optimal but feasible solution in a reasonable computation time.

B. ADMM Algorithm Modifications

As explained in [31], the general form of ADMM is presented for two blocks of functions and variables. However, the present problem has as many blocks as prosumers in the portfolio. This is important to ensure privacy of end-users information. References [31] and [41] present two modifications to the original ADMM. First, they suggested to update the primal variables concurrently as the sequential variable update would slow down obtaining the solution. Otherwise, every prosumer should wait for the variable update of its

Algorithm 2: Two-Steps Fast-PJ-ADMM for Optimal Flexibility Provision

```

1 Initialize:  $x_i^{(0)}, \rho^{(0)} > 0, \lambda_t^{(0)} = 0$ ;
   Input:  $K^i, K^d, \epsilon^{pri}, \epsilon^{dual}, \tau^{incr}, \tau^{decr}, CT^{max}, k^{max}, W^{flex}$ 
2 while  $\epsilon^{pri} > \|r_t^k\|_2$  and  $\epsilon^{dual} > \|s_t^k\|_2$  do
3   for  $i=1,2,\dots,I$  do
4     ( $x_i$  is updated concurrently);
5      $x_i^{(k+1)} := \operatorname{argmin}_{x_i}$ 
6        $\mathcal{L}_\rho(x_i, x_{j \neq i}^k, \lambda_t^k, \rho^{(k+1)}) + \frac{1}{2} \|x_i - x_i^{(k)}\|_{P_i}^2$ ;
7       s.t. Site  $i$  constraints: (1b)(1c)(1d)(1e)
8   end
9   Update dual and penalty variables ;
10  if  $\|r_t^{(k)}\|_2 > 0.05 \|FR_t\|_2$  then
11    Fast update:  $\rho^{(k+1)}$  according to (7);
12    Update  $\lambda_t^{(k+1)} := \lambda_t^k + \gamma \rho^{(k+1)} r_t^{(k+1)}, \forall t \in \mathcal{T}^\pm$ ;
13  else
14    Soft update:  $\lambda_t^{(k+1)}$  according to (9)
15  end
16 Update  $\|r_t^{(k)}\|_2, \|s_t^{(k)}\|_2, k = k + 1$ 

```

neighbour before calculating the optimal solution. This allows for a larger problem dimension since it can be solved in a distributed computing system concurrently. Also, it reduces the computational cost as the parallelization gains overcome the overhead derived from it. Second, they introduce the Proximal Jacobian (PJ) regularization term ($\frac{1}{2} \|x_i - x_i^{(k)}\|_{P_i}^2$), which preserves parallel updating. The norm of this term is defined as $\|x_i\|_{P_i}^2 = x_i^T P_i x_i$ with $P_i = Id$. It guarantees strong convexity of the problem and enhances stability. The damping parameter γ is set to 1.5 as suggested in [31].

C. Penalty Parameter and Dual Variables Updating

Algorithm 2 illustrates the dual update accelerated iteration process divided in two steps.

1) *Step 1—Fast Updating*: the early iterations (k) are accelerated by varying the penalty parameter $\rho^{(k)}$ according to (7) as per the approach adapted by [23]. τ^{incr} and τ^{decr} are increasing and decreasing factors in order to speed up the algorithm. $\rho^{(k)}$ is used to update dual variables $\lambda_t^{(k+1)}$ according to (8a), (8b) is the primal residual, and (8c) is the dual residual. $r_t^{(k)}$ is positive when the set of prosumer sites I cannot provide enough up-regulation to meet the FR at iteration k and dual variable $\lambda_t^{(k)}$. Otherwise, $r_t^{(k)}$ is negative.

$$\rho^{(k+1)} := \begin{cases} \tau^{incr} \rho^{(k)} & \text{if } \|r^{(k)}\|_2 > \mu \|s^{(k)}\|_2 \\ \rho^{(k)} / \tau^{decr} & \text{if } \|s^{(k)}\|_2 > \mu \|r^{(k)}\|_2 \\ \rho^{(k)} & \text{otherwise,} \end{cases} \quad (7)$$

$$\lambda_t^{(k+1)} := \lambda_t^{(k)} + \gamma \rho^{(k)} r_t^{(k)} \quad \forall t \in \mathcal{T}^\pm \quad (8a)$$

$$r_t^{(k)} = \sum_{i \in \mathcal{I}} \left(\chi_{p,t}^{tot,(k)} - W_t^{flex} \right) \quad \forall t \in \mathcal{T}^\pm \quad (8b)$$

$$s_t^{(k)} = r_t^{(k)} - r_t^{(k-1)} \quad \forall t \in \mathcal{T}^\pm. \quad (8c)$$

2) *Step 2—Soft Updating*: the dual update changes to (9) at iteration k^* once the primal error is equal or less than threshold value like 5% of the FR. Then, it starts collecting accumulated primal error over iterations from k^* to k and includes integration and dual residual regulation parameters K^i and K^d inspired in classic control theory [42]. They allow to better regulate the dual variables update and damp oscillations in the error and objective function along the iterative solution process. However, at this moment it is unclear how to tune the parameters to accelerate the convergence. It is to be noted that penalty parameter $\rho^{(0)}$ is the initial value.

$$\lambda_t^{(k+1)} := \lambda_t^{(k)} + \gamma \rho^{(0)} r_t^{(k)} + K^i \sum_{i=k^*}^k r_t^{(i)} + K^d s_t^{(k)} \quad \forall t \in \mathcal{T}^\pm \quad (9)$$

The algorithm stops when the norm of the primal and dual residuals are both smaller than some given thresholds (ϵ^{pri} and ϵ^{dual} respectively). Additionally, a maximum number of iterations k^{max} and computational time (CT^{max}) are specified as well. Depending on the requirements of the case, it might be interesting to compute as many iterations as possible in a pre-specified time, or on the contrary run for as long as needed the algorithm until we reach a precision requirement. Both scenarios are tested in Section VII experiments.

VI. CASE STUDY

The case study considered for analysis consists of 100 domestic houses which have photovoltaic panels installed and their historic measurement data are available through the Dataport [43]. The household consumption data and PV generation data considered for the case study are for the date June the 28th of 2018 because the consumption and PV generation were significantly high. The electricity price is from the Spanish day-ahead market price for the same day in combination with the Spanish two-periods grid tariff which has valley hours from 11 pm until 13 pm on the next day (14 hours) and the rest of the hours are considered as peak hours for summer period. Metering and forecasted values have hourly resolution and the optimization horizon is one day. The optimization process is assumed to be executed at 11:45 pm each day and takes decisions based on the load and PV power production forecast for each site. For simplicity, the study considers only one FR which is for one period (1 hour).

The simulation set-up will be complete by adding a battery to each household, which is the flexibility source and the battery model is explained in the the Appendix. Battery parameters for the case study are the investment cost which is EUR 3,000 for the first site and it is increased in steps of 1% for the successive sites. Moreover, batteries' maximum charging and discharging power are 3.8 kW and capacity is 10 kWh for all batteries. Battery converter parameters and efficiency are taken from technical data sheet of SMA-SBS3.7-10 converter by assuming the average operational voltage is $V_{DC} = 550$ V [44]. The diversity in the battery technology and their ageing in the considered population of 100 batteries are also represented by their efficiency. The battery efficiency

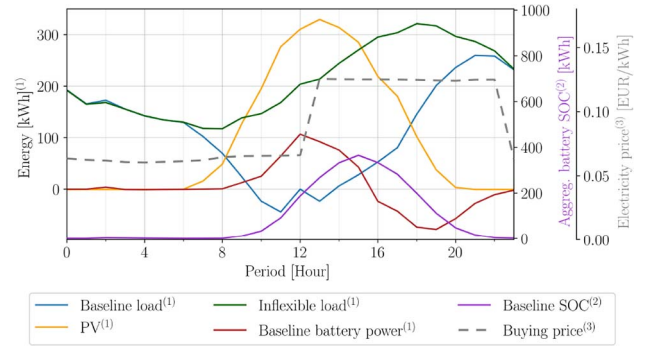


Fig. 2. Aggregated results of the site level optimization problem (1).

for the first site is considered as 98% and the battery efficiency in the successive households are reduced in steps of 0.1%. The values used for constant voltage charging parameter and calendar ageing related parameters are as follows $W_i^{bat} = 0.2$, $S_i^{LT} = 10$ years, $S_i^0 = 0.3$ and $S_i^{SOC} = 1.7$ according to [45], [46], and they are the same for all battery units. The cycle ageing model considers the battery as 10 segments.

The FR in this case study is formulated to reduce the evening peak at 8 pm according to the local DSO needs. Though the household consumption shows a peak at 10 pm, the network congestion can happen at hours other than hours at which the households portfolio shows a peak. Therefore, the present case study does not cut the portfolio peak as it is not the purpose of the present flexibility service provision.

VII. RESULTS

A. Site Level Optimization

In site level optimization, every individual prosumer is optimized to achieve low energy cost independent from others. Fig. 2 shows the aggregated results of problem (1). Results show that batteries are partially charged during the afternoon to store the PV power production surplus and they are discharged during the evening. This phenomenon is due to calendar ageing penalty, batteries tend to charge at the latest possible low priced period to reduce the time between charge and discharge. In addition, the cycling and calendar ageing factors prevent to charge and discharge batteries for arbitrage as the economic margin does not surpass the battery degradation costs. It is noticeable that some PV systems are oversized. As there is not enough load during sunny hours or battery capacity, the baseline load shows some periods with net aggregated export of energy.

B. Centralised Flexibility Provision

This section shows the results of centralised ALFO and ALFM algorithms for the described case study. The available flexibility is calculated by the ALFO problem (2). The FR is for 400 kWh at 8 pm and the households portfolio provides 308.86 kWh as the maximum available flexibility. Aggregator cannot provide more flexibility as some battery discharges are already scheduled by the site optimization problem (1). Fig. 3 shows the increase in battery charging during the hours before

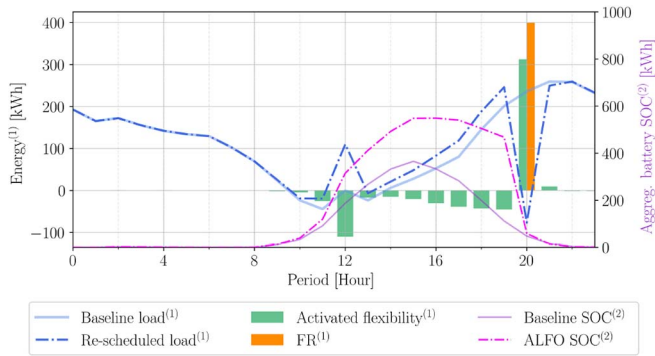


Fig. 3. ALFO problem results of re-scheduling of 100 sites and batteries under a FR of 400 kWh.

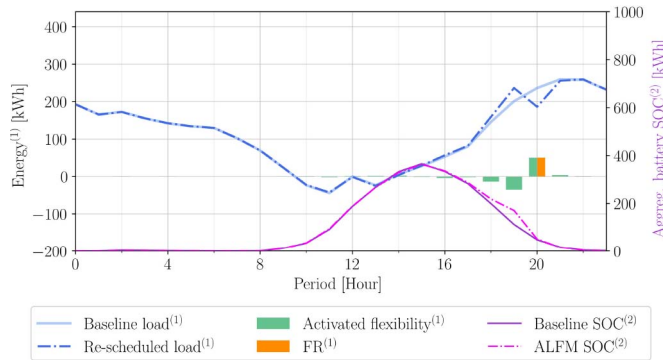


Fig. 4. ALFM problem results under a FR of 50 kWh of 100 sites.

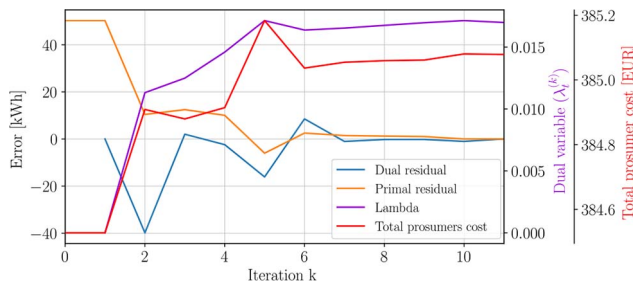


Fig. 5. Comparison of errors, total prosumers costs and dual variable per iteration of Algorithm 2 with $K^i = 2 \cdot 10^{-4}$ and $K^d = 5 \cdot 10^{-7}$.

FR to charge all batteries sufficiently for latter discharge at 8 pm during FR.

Afterwards, the accepted FR is 50 kWh (lower than the available maximum flexibility). Therefore, the ALFM step (4) is executed to re-schedule batteries to meet the accepted FR. Fig. 4 shows the new feasible solution for the accepted FR at minimum cost for all sites. The complexity of the case study is the significant number of possibilities to attend the accepted FR as the it represents 17% of the portfolio available flexibility. From computational point of view, the accepted FR constitutes a complicated case as many combinations of batteries could satisfy constraint (4b) at similar cost.

C. Distributed Flexibility Provision

The proposed distributed ADMM Algorithm 2 is tested with the same case study compared with centralised algorithm.

Fig. 5 shows the primal and dual errors, dual variable $\lambda_t^{(k)}$ and the total prosumer cost converge for 11 iterations. The rate of change of primal error in successive iterations is high till the iteration $k = 5$. After that, the error variation is low. This phenomenon is due the fast dual variable updating according to (8a) when error is lower than 5% of FR. Thereafter, the soft updating is activated and it changes error rate smoothly by avoiding large variations. The initial value of $\lambda_t^{(0)}$ at zero provides a solution which corresponds to the site optimization result. When Algorithm 2 updates $\lambda_t^{(k)}$, the portfolio tends to increase flexibility provision and the primal error decreases. The solution is found in less than 5 minutes and the memory usage is very low (around 200 MB) as each iteration is a separated optimization problem per site and the memory contents are flushed after each iteration.

D. Scalability Analysis

Regarding scalability limitations, the centralised algorithms using the Gurobi solver with the branch-and-bound and the dual simplex algorithms, they consume the maximum available RAM memory of 16 GB for the 100 sites case study and takes approximately 1 hour to solve the ALFO problem and around 20 minutes for the ALFM problem on high performance computer with AMD Ryzen Threadripper 16 Core Processor running at 3.5 GHz. The ALFO problem takes more time due to the quadratic flexibility penalty term in the objective function. Fig. 6 shows that the Fast-PJ-ADMM Algorithm 2 which finds solutions at similar duration in comparison with ALFM and ALFO problems in the case with 50 sites but centralised algorithms take between 5 and 12 folds more time for the 100 sites case. Therefore, there is a scalability limit to solve large-scale flexibility problems with complicating constraints (2b), (2c), (4b), (4c), and detailed battery models using centralised algorithms.

From a theoretical perspective the situation is the following. As the complexity of the model increases by including more sites, the centralised algorithms begin to suffer because of the exponential increase of paths within the binary variable decision tree. Additionally, these algorithms are not parallelisable due to intrinsic limitations. The ADMM parallelisation solves these two issues. First, it limits the size of each decision tree by restricting the binary variables to those corresponding to that particular site. Additionally, it enables to solve each site independently by applying the original centralised algorithm now to a problem several orders of magnitude smaller. We claim that this solution is scalable since individual site problems remain of constant size independently of the number of sites in the general problem.

E. Distributed Algorithm Acceleration Comparison

This section discusses around four versions of the ADMM algorithms previously presented in the literature namely Regular (original algorithm [23]), Fast (acceleration via penalty parameter [23]), PJ (parallelized, regularized version [41]), and Fast-PJ (combination of acceleration, parallelization, and regularization), and the novel version Two-steps Fast-PJ Algorithm 2 by comparing the way penalty parameter ($\lambda_t^{(k)}$) is

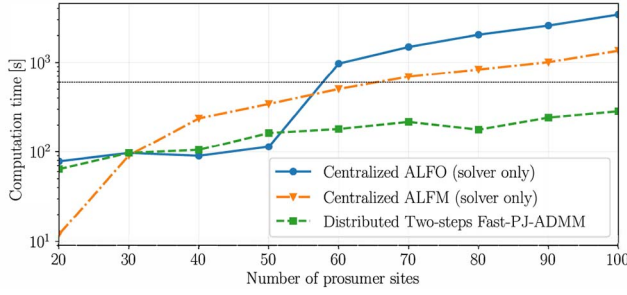


Fig. 6. Computational cost comparison of ALFO, ALFM and Fast-PJ-ADMM Algorithm 2. Horizontal dashed line highlights 10 minutes computation time threshold.

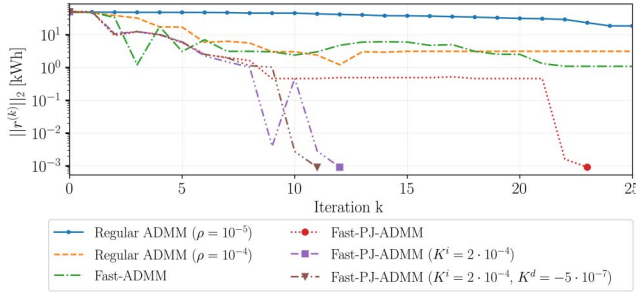


Fig. 7. Primal error comparison of different acceleration algorithms under a FR at 8 pm of 50 kWh in a portfolio of 100 sites including the soft updating in all algorithms when $r^{(k)} = 2.5$ kWh. Markers indicate when algorithms meet $\epsilon^{pri} = \epsilon^{dual} = 10^{-3}$.

updated for the optimal flexibility exchange problem in each algorithm. Therefore, it is possible to see the impact of acceleration, parallelization, regularization and the two-step algorithm modifications. All accelerated algorithms begin with the same penalty parameter value ($\rho^{(0)} = 10^{-4}$) and they continue with the soft update when $\|r_i^{(k)}\|_2$ and $\|s_i^{(k)}\|_2 \leq 0.05$ kWh.

Fig. 7 shows a comparison of absolute primal error values change per iteration of different distributed optimization algorithms. It is to be noted that the absolute error value hide cases when primal errors varies between positive and negative values as shown in Fig. 5. Although they are reaching the same optimal cost, the regular ADMM with $\rho = 10^{-5}$ takes 20 iterations to find a solution with primal error $r_i^{(k)} = 20$ kWh, and 200 iterations for 1% error. In case of increasing the penalty parameter to $\rho = 10^{-4}$, the regular ADMM performance differs from the previous case near sub-optimal solutions from $k=4$. This phenomenon is due to the drastic change in dual update. The regular ADMM and all the following algorithms proved to provide better solutions if they use an initial value for dual variable as $\lambda_i^{(0)} = 0$. Thus, the performance of the algorithm differs from no flexibility provision to the optimal battery schedule to provide full FR.

The Fast-ADMM changes the penalty parameter according to (7) using the following acceleration parameters: $\tau^{incr} = 1.5$, $\tau^{decr} = 2$ and $\mu = 2$. In all accelerated algorithms, dual variable λ_i changes at a higher rate between successive iterations until iteration $k=5$ where they reach a primal error equal or lower than 5% of FR ($\|r_i^{(k)}\|_2 = 2.5$ kWh). Thereafter, their performance differs from each other around the optimal solution. The inclusion of the PJ regularization term in the Algorithm 2 according to [31] allows to stabilize the objective

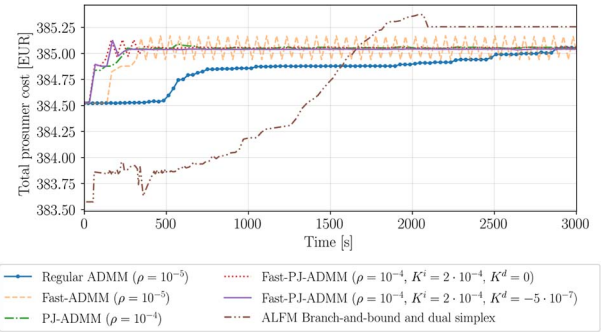


Fig. 8. Prosumer total cost over computation time of centralised and distributed algorithms with FR=50 kWh and $\epsilon^{pri} = \epsilon^{dual} = 10^{-5}\%$.

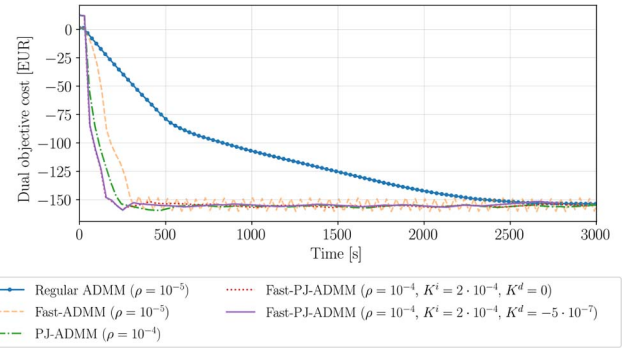


Fig. 9. Dual objective cost over computation time of distributed algorithms with FR=50 kWh and $\epsilon^{pri} = \epsilon^{dual} = 10^{-5}\%$.

function and it finds an optimal solution with 2% error in 9 iterations. Additionally, it finds an optimal solution ($\epsilon^{pri} < 10^{-3}\%$) in 24 iterations if parameters are $\rho^{(0)} = 10^{-4}$ and $K^d = K^i = 0$ during the soft update. In contrast to the previous algorithms, Fast-PJ-ADMM Algorithm 2 with $K^i = 2 \cdot 10^{-4}$ and $K^d = -5 \cdot 10^{-7}$ finds the optimal solution in 11 iterations. The effect of K^i is to faster approach to the objective function expected value and K^d smooths variations.

Fig. 8 shows the total prosumer cost variation over the resolution time of centralised and multiple distributed algorithms. This cost corresponds to the primal objective without the dual objective in order to compare the ADMM results with the ALFM branch-and-bound and dual simplex algorithm. Moreover, the ADMM results tend to increase from the starting point as the initial dual variable (λ_i) is initiated with null value. All methods find very similar solutions but they approach to the objective value differently. The centralised ALFM algorithm takes 2,000 seconds before reaching a feasible solution. In contrast, most of distributed algorithms find a suitable solution in less than 200 seconds. Notice the Regular ADMM takes 3,000 seconds to reach the optimal value and the Fast ADMM varies around the optimal solution. The PJ regularization term reduces variations and the K^i and K^d parameters allow to accelerate the path to the optimal objective cost without creating variations in the objective function. The reader can observe that the starting point of ADMM algorithms is close to the primal final objective. However, Fig. 7 shows this is not a valid solution. Additionally, it is relevant to mention that the initial point, when $\lambda_i^{(k=0)}$, is equivalent to the site optimization problem (1) which is previously calculated and the addition

of the FR in the problem is not significant in terms of the primal objective. However, the dual objective changes significantly as Fig. 9 shows. In the case of the regular ADMM it takes more than 2,000 seconds to convergence. Regarding modified ADMM algorithms, Fast and PJ-ADMM algorithms accelerate their convergence and Fast-PJ-ADMM algorithms get stable in less than 500 seconds.

VIII. CONCLUSION

The present paper presents a novel formulation to optimize the operation of distributed storage units behind-the-meter to provide flexibility services to a balance responsible party or distribution system operator. In this context, an aggregator manages a group of prosumers with storage units who are willing to participate in the local flexibility market. In addition, this paper includes the decomposed optimization problem formulation for large-scale portfolios using a modified accelerated PJ-ADMM algorithm divided in two steps: fast and soft dual variable updating. The fast and soft updating accelerate the iterative process reducing variations in the dual variable and objective functions. The soft update might be relevant for case studies with binary variables as dual errors can be zero although the dual variable changes. Case study results show that this formulation is best suited for large scale implementations as it can find aggregated optimal solutions faster by considering local constraints and prices with the appropriate parameters tuning. The results also highlight that the centralised and distributed methods find very similar solutions but the distributed one can overcome the scalability limitations. For instance, the case study shows a break-even point at 50 prosumer sites when the distributed algorithm is less computationally demanding than the centralised. In future, the performance of the proposed decomposition algorithm can be tested by including other flexibility device models such as electric water heaters or electric vehicles which may increase the complexity of their aggregated optimization. Additionally, the two-step Fast-PJ-ADMM algorithm can be applied for scheduling FDs in peer-2-peer local markets to find optimal exchanges even without an aggregator as a manager of the energy community. However, the aggregator role could reduce the number of exchanged messages between BRP/DSO and peers. Therefore, possibility of decentralised local market without aggregator is considered for further work.

APPENDIX STATIONARY BATTERY MODEL

This Appendix provides the stationary battery model used in the present paper. The elemental battery state-of-charge (SOC) evolution constraint of prosumer site i is shown in (10a). Battery SOC has upper (O_i^{max}) and lower boundaries (O_i^{min}), and charging and discharging power limits are (Q_i^{ch}) and (Q_i^{dis}).

$$\begin{aligned} \sigma_{i,t}^{SOC} = & \sigma_{i,t-1}^{soc} + \sigma_{i,t}^{ch} A_i^{bat,ch} a^{inv,ch} \\ & - \frac{\sigma_{i,t}^{dis}}{A_i^{bat,dis} a^{inv,dis}} \quad \forall i, t \end{aligned} \quad (10a)$$

$$O_i^{min} \leq \sigma_{i,t}^{SOC} \leq O_i^{max} \quad \forall i, t \quad (10b)$$

$$\sigma_{i,t}^{ch} \leq Q_i^{ch} \delta_{i,t}^{bat} \quad \forall i, t \quad (10c)$$

$$\sigma_{i,t}^{dis} \leq Q_i^{dis} (1 - \delta_{i,t}^{bat}) \quad \forall i, t \quad (10d)$$

Because batteries are expensive and suffer from higher rate of degradation under heavy stress [46], an advanced battery model has been developed in order to make more accurate decisions. The developed battery model is formulated by including battery degradation cost in such a way to reflect real costs of operation as closely as possible to reality while maintaining the computational burden at an acceptable level. The battery model has 4 main attributes in addition to the simple model which are cycle and calendar degradations, power limitations when approaching fully charged and fully discharged states to avoid reaching the voltage limits, and piecewise linearized inverter efficiency. The following section describes these attributes in detail.

1) *Cycle Degradation*: The most common stationary batteries at end-user level today are lithium ion batteries, typically li-ion nickel-manganese-cobalt (LI-NMC) batteries. The degradation factors of such batteries are predominantly depending on charge-discharge cycle depth during operation. Therefore, the lifetime of these batteries depends on the depth and number of cycles. In addition, shallow cycles have significantly lower degradation cost than deep ones. A detailed cycle degradation model is presented in [39]. The cycle degradation model factorizes the cycle depth and accounts degradation as a cost of discharging the battery with a certain depth. In order to keep track of the depth-of-discharge, the battery model adds virtual segments indexed by j as presented in [39]. (11a) tracks the segmented SOC evolution given segmented variables, whereas (11b) restrains the maximum energy per segment. (11c) and (11d) sums the power in all segments j to equal the original variables. Finally, (11e) calculates the degradation cost as function of discharge power.

2) *Calendar Ageing*: The calendar ageing is modelled as a function of SOC dependent cost per time period, as shown in (12). The core idea is that calendar based degradation cost increases with higher SOC and it incentives the battery to stay at a low SOC when not utilized. The tuning factors S_i^0 and S_i^{SOC} implicate how much the calendar ageing depends on SOC as described in [45].

3) *Constant - Voltage Charging/Constant - Current Discharging*: The constant-voltage charging and constant-current discharging regions of a battery does not apply to the full SOC area of a battery. (13a) and (13b) reduces the allowed charging and discharging power when approaching the maximum and minimum energy levels respectively.

$$\begin{aligned} \sigma_{i,t,j}^{seg,SOC} = & \sigma_{i,t,j}^{seg,ch} A^{bat,ch} a^{inv,ch} (\sigma_{i,t,j}^{seg,ch}) \\ & + \frac{\sigma_{i,t,j}^{seg,dis}}{A^{bat,dis} a^{inv,dis} (\sigma_{i,t,j}^{seg,dis})} + \sigma_{i,t-1,j}^{seg,SOC} \quad \forall i, t \end{aligned} \quad (11a)$$

$$\sigma_{i,t,j}^{seg,SOC} \leq O_{i,j}^{seg,max} \quad \forall i, j, t \quad (11b)$$

$$\sigma_{i,t}^{ch} = \sum_{j \in \mathcal{J}} \sigma_{i,t,j}^{seg,ch} \quad \forall i, t \quad (11c)$$

$$\sigma_{i,t}^{dis} = \sum_{j \in \mathcal{J}} \sigma_{i,t,j}^{seg,dis} \quad \forall i, t \quad (11d)$$

$$\beta_{i,t}^{cyc} = \sum_{j \in \mathcal{J}} C_{i,j} \sigma_{i,t,j}^{seg,dis} \quad \forall i, t \quad (11e)$$

$$\beta_{i,t}^{cal} = \frac{C_i^{bat}}{S_i^{LT}} \cdot \left(S_i^0 + \frac{1}{2} S_i^{SOC} \cdot (\sigma_{i,t}^{SOC} + \sigma_{i,t-1}^{SOC}) \right) \forall i, t \quad (12)$$

$$\sigma_{i,t}^{ch} \leq \frac{O_i^{max} - \sigma_{i,t-1}^{SOC}}{(1 + W_i^{bat})} \quad \forall i, t \quad (13a)$$

$$\sigma_{i,t}^{dis} \leq \frac{\sigma_{i,t-1}^{SOC} - O_i^{min}}{(1 + W_i^{bat})} \quad \forall i, t. \quad (13b)$$

4) *Piecewise Linearised Inverter Efficiency*: The total storage system efficiency is a combination of two factors, the inverter efficiency ($a^{inv,ch}, a^{inv,dis}$) and the battery efficiency ($A^{bat,ch}, A^{bat,dis}$). A piecewise linearized approach is chosen in order to capture the power dependency of inverter efficiency. At low input power inverter efficiency is very low, on the other hand the efficiency reaches 98% at high input power. The piecewise linearisation is modelled using a special order sets of type 2 (SOS2) approach to approximate the non-linear dependency on input power. This approach adds four additional binary variables per time step (two for charging, two for discharging) to the problem, and is one of the preferred methods first developed in [47].

ACKNOWLEDGMENT

The authors thank Pecan Street, Inc. for allowing access to its DataPort database. E. Prieto is lecturer of the Serra Hünter programme.

REFERENCES

- [1] *INVADE H2020 Website*. Accessed: Feb. 17, 2019. [Online]. Available: <https://h2020invade.eu/>
- [2] M. van den Berge, M. Broekmans, B. Derksen, A. Papanikolaou, and C. Malavazos, "Flexibility provision in the smart grid era using USEF and OS4ES," in *Proc. IEEE Int. Energy Conf.*, Apr. 2016, pp. 1–6.
- [3] M. Beaudin and H. Zareipour, "Home energy management systems: A review of modelling and complexity," *Renew. Sustain. Energy Rev.*, vol. 45, pp. 318–335, May 2015.
- [4] B. Zhou *et al.*, "Smart home energy management systems: Concept, configurations, and scheduling strategies," *Renew. Sustain. Energy Rev.*, vol. 61, pp. 30–40, Aug. 2016.
- [5] Q. Wang, C. Zhang, Y. Ding, G. Xydis, J. Wang, and J. Østergaard, "Review of real-time electricity markets for integrating distributed energy resources and demand response," *Appl. Energy*, vol. 138, pp. 695–706, Jan. 2015.
- [6] A. Dietrich and C. Weber, "What drives profitability of grid-connected residential PV storage systems? A closer look with focus on Germany," *Energy Econ.*, vol. 74, no. 2018, pp. 399–416, 2018.
- [7] K. Spiliotis, A. I. R. Gutierrez, and R. Belmans, "Demand flexibility versus physical network expansions in distribution grids," *Appl. Energy*, vol. 182, pp. 613–624, Nov. 2016.
- [8] J. Varela, N. Hatziaargyriou, L. J. Puglisi, M. Rossi, A. Abart, and B. Bletterie, "The IGREENGrid project: Increasing hosting capacity in distribution grids," *IEEE Power Energy Mag.*, vol. 15, no. 3, pp. 30–40, May/June 2017.
- [9] C. Eid, P. Codani, Y. Perez, J. Reneses, and R. Hakvoort, "Managing electric flexibility from distributed energy resources: A review of incentives for market design," *Renew. Sustain. Energy Rev.*, vol. 64, pp. 237–247, Oct. 2016.
- [10] A. M. Carreiro, H. M. Jorge, and C. H. Antunes, "Energy management systems aggregators: A literature survey," *Renew. Sustain. Energy Rev.*, vol. 73, pp. 1160–1172, Jun. 2017.
- [11] S. Ø. Ottesen, A. Tomasgard, and S. E. Fleten, "Multi market bidding strategies for demand side flexibility aggregators in electricity markets," *Energy*, vol. 149, pp. 120–134, Apr. 2018.
- [12] S. Burger, J. P. Chaves-Ávila, C. Battle, and I. J. Pérez-Arriaga, "A review of the value of aggregators in electricity systems," *Renew. Sustain. Energy Rev.*, vol. 77, pp. 395–405, Feb. 2016.
- [13] I. Kim, "A case study on the effect of storage systems on a distribution network enhanced by high-capacity photovoltaic systems," *J. Energy Storage*, vol. 12, pp. 121–131, Aug. 2017.
- [14] M. Resch, J. Bühler, B. Schachler, R. Kunert, A. Meier, and A. Sumper, "Technical and economic comparison of grid supportive vanadium redox flow batteries for primary control reserve and community electricity storage in Germany," *Int. J. Energy Res.*, vol. 43, no. 1, pp. 337–357, 2019.
- [15] O. Alrumayh and K. Bhattacharya, "Flexibility of residential loads for demand response provisions in smart grid," *IEEE Trans. Smart Grid*, vol. 10, no. 6, pp. 6284–6297, Nov. 2019.
- [16] S. Hu *et al.*, "Agent-based coordinated operation strategy for active distribution network with distributed energy resources," *IEEE Trans. Ind. Appl.*, vol. 55, no. 4, pp. 3310–3320, Jul./Aug. 2019.
- [17] H. Zoeller, M. Reischboeck, and S. Henselmeyer, "Managing volatility in distribution networks with active network management," in *Proc. CIRED Workshop*, 2016, pp. 1–4.
- [18] "Smart grid traffic light concept design of the amber phase discussion Paper," German Assoc. Energy Water Ind., BDEW, Berlin, Germany, Rep., Mar. 2015.
- [19] T. Sousa, F. Lezama, S. Ramos, and Z. Vale, "A flexibility home energy management system to support aggregator requests in smart grids," in *Proc. IEEE Symp. Comput. Intell.*, 2018, pp. 1830–1836.
- [20] S. S. Torbaghan *et al.*, "A market-based framework for demand side flexibility scheduling and dispatching," *Sustain. Energy Grids Netw.*, vol. 14, pp. 47–61, Jun. 2018.
- [21] S. Vandael, B. Claessens, M. Hommelberg, T. Holvoet, and G. Deconinck, "A scalable three-step approach for demand side management of plug-in hybrid vehicles," *IEEE Trans. Smart Grid*, vol. 4, no. 2, pp. 720–728, Jun. 2013.
- [22] F. L. Müller, J. Szabó, O. Sundström, and J. Lygeros, "Aggregation and disaggregation of energetic flexibility from distributed energy resources," *IEEE Trans. Smart Grid*, vol. 10, no. 2, pp. 1205–1214, Mar. 2019.
- [23] S. Boyd, N. Parikh, E. Chu, B. Peleato, J. Eckstein, and Others, "Distributed optimization and statistical learning via the alternating direction method of multipliers," *Found. Trends Mach. Learn.*, vol. 3, no. 1, pp. 1–122, 2011.
- [24] T. Erseghe, "Distributed optimal power flow using ADMM," *IEEE Trans. Power Syst.*, vol. 29, no. 5, pp. 2370–2380, Sep. 2014.
- [25] V. Dvorkin, J. Kazempour, L. Baringo, and P. Pinson, "A consensus-ADMM approach for strategic generation investment in electricity markets," in *Proc. IEEE Conf. Decis. Control*, 2018, pp. 780–785.
- [26] Q. Zhang, K. Dehghanpour, and Z. Wang, "Distributed CVR in unbalanced distribution systems with PV penetration," *IEEE Trans. Smart Grid*, vol. 10, no. 5, pp. 5308–5319, Sep. 2019.
- [27] R. R. Nejad and W. Sun, "Distributed load restoration in unbalanced active distribution systems," *IEEE Trans. Smart Grid*, vol. 10, no. 5, pp. 5759–5769, Sep. 2019.
- [28] R. R. Nejad, W. Sun, and A. Golshani, "Distributed restoration for integrated transmission and distribution systems with DERs," *IEEE Trans. Power Syst.*, vol. 34, no. 6, pp. 4964–4973, Nov. 2019.
- [29] J. Brooks, W. Hager, and J. Zhu, "A decentralized multi-block ADMM for demand-side primary frequency control using local frequency measurements," 2015. [Online]. Available: [arXiv:1509.08206](https://arxiv.org/abs/1509.08206).
- [30] D. H. Nguyen, S. Azuma, and T. Sugie, "Novel control approaches for demand response with real-time pricing using parallel and distributed consensus-based ADMM," *IEEE Trans. Ind. Electron.*, vol. 66, no. 10, pp. 7935–7945, Oct. 2019.
- [31] L. Liu and Z. Han, "Multi-block ADMM for big data optimization in smart grid," in *Proc. Int. Conf. Comput. Netw. Commun. (ICNC)*, 2015, pp. 556–561.
- [32] W. Deng, M.-J. L. Zhimin, and W. Yin, "Parallel multi-block ADMM with o(1/k) convergence," *J. Sci. Comput.*, vol. 71, no. 2, pp. 712–736, 2017.
- [33] T. Sousa, T. Soares, P. Pinson, F. Moret, T. Baroche, and E. Sorin, "Peer-to-peer and community-based markets: A comprehensive review," *Renew. Sustain. Energy Rev.*, vol. 104, pp. 367–378, Apr. 2019.

- [34] T. Baroche, P. Pinson, R. L. G. Latimier, and H. B. Ahmed, "Exogenous cost allocation in peer-to-peer electricity markets," *IEEE Trans. Power Syst.*, vol. 34, no. 4, pp. 2553–2564, Jul. 2019.
- [35] F. Moret and P. Pinson, "Energy collectives: A community and fairness-based approach to future electricity markets," *IEEE Trans. Power Syst.*, vol. 34, no. 5, pp. 3994–4004, Sep. 2019.
- [36] G. Liu, T. Jiang, T. B. Ollis, X. Zhang, and K. Tomovic, "Distributed energy management for community microgrids considering network operational constraints and building thermal dynamics," *Appl. Energy*, vol. 239, pp. 83–95, Apr. 2019.
- [37] P. Olivella-Rosell *et al.*, "Local flexibility market design for aggregators providing multiple flexibility services at distribution network level," *Energies*, vol. 11, no. 4, p. 822, 2018.
- [38] K. Kok and S. Widergren, "A society of devices: Integrating intelligent distributed resources with transactive energy," *IEEE Power Energy Mag.*, vol. 14, no. 3, pp. 34–45, May/June 2016.
- [39] B. Xu, J. Zhao, T. Zheng, E. Litvinov, and D. S. Kirschen, "Factoring the cycle aging cost of batteries participating in electricity markets," *IEEE Trans. Power Syst.*, vol. 33, no. 2, pp. 2248–2259, Mar. 2018.
- [40] P. Lloret-Gallego and P. Olivella-Rosell, *INVADE D4.3 Overall INVADE Architecture Final*, Universitat Politècnica de Catalunya, Barcelona, Spain, Rep., 2018.
- [41] M. Ma, L. Fan, and Z. Miao, "Consensus ADMM and proximal ADMM for economic dispatch and AC OPF with SOCP relaxation," in *Proc. IEEE 48th North Amer. Power Symp. Process (NAPS)*, 2016, pp. 1–6.
- [42] B. C. Kuo and F. Golnaraghi, *Automatic Control Systems*, vol. 9. Englewood Cliffs, NJ, USA: Prentice-Hall, 1995.
- [43] Pecan Street Inc. *Dataport*. Accessed: Jan. 7, 2019. [Online]. Available: <https://dataport.cloud/>
- [44] "Technical information. Efficiency and derating. Sunny boy storage, version 4.6," SMA Solar Technol. AG, Niestetal, Germany, Rep., 2019.
- [45] A. Hentunen, J. Forsström, and V. Mukherjee, "INVADE D6.5 advanced battery techno-economics tool," VTT Tech. Res. Centre Finland Ltd., Espoo, Finland, Rep., 2018.
- [46] M. Ecker *et al.*, "Calendar and cycle life study of Li(NiMnCo)O₂-based 18650 lithium-ion batteries," *J. Power Sources*, vol. 248, pp. 839–851, Feb. 2014.
- [47] E. M. L. Beale and J. J. H. Forrest, "Global optimization using special ordered sets," *Math. Program.*, vol. 10, no. 1, pp. 52–69, 1976.

Pol Olivella-Rosell (Student Member, IEEE) received the M.Sc. degree in industrial engineering from the School of Industrial Engineering of Barcelona, Universitat Politècnica de Catalunya (UPC), Barcelona, Spain, in 2013, where he is currently pursuing the Ph.D. degree in electrical engineering. Since 2011, he has been with the CITCEA-UPC Research Group. His research interests include power systems, local electricity markets, optimization and demand response.

Francesc Rullan (Student Member, IEEE) received the M.Sc. degrees in mathematics and telecommunications engineering from the Interdisciplinary Higher Education Centre, Universitat Politècnica de Catalunya. He is currently pursuing the Ph.D. degree with the Centre for Medical Imaging Computing, University College London. His research interests include numerical resolution of partial differential equations, inverse problems applied to medical imaging, and numerical optimization.

Pau Lloret-Gallego received the M.Sc. degree in industrial engineering from the School of Industrial Engineering of Barcelona, Universitat Politècnica de Catalunya (UPC), Barcelona, Spain, in 2006. Since 2004, he has been with CITCEA-UPC Research Group. His research interests include smart grids, local electricity markets, optimization, and demand response.

Eduardo Prieto-Araujo (Member, IEEE) received the M.Sc. degree in industrial engineering from the School of Industrial Engineering of Barcelona, and the Ph.D. degree in electrical engineering from the Universitat Politècnica de Catalunya (UPC), Barcelona, Spain, in 2011 and 2016, respectively. In 2010, he joined CITCEA-UPC Research Group, where he is currently a Serra Hünter Lecturer with the Electrical Engineering Department. His main interests are renewable generation systems, control of power converters for HVDC applications, interaction analysis between converters, and power electronics dominated power systems.

Ricard Ferrer-San-José (Student Member, IEEE) received the M.Sc. degree in industrial engineering from the School of Industrial Engineering of Barcelona, Universitat Politècnica de Catalunya (UPC), Barcelona, Spain, in 2015, where he is currently pursuing the Ph.D. degree in electrical engineering. Since 2013, he has been with the CITCEA-UPC research group where he has been focused on different research topics, such as power electronic dominated power systems, PV and wind generation integration, and HVDC.

Sara Barja-Martínez received the M.Sc. degree in industrial engineering from the School of Industrial Engineering of Barcelona, Universitat Politècnica de Catalunya (UPC), Barcelona, Spain, in 2018, where she is currently pursuing the Ph.D. degree in electrical engineering. Since 2017, she has been with the CITCEA-UPC research group. Her research interests include energy management system algorithms, flexibility markets, optimization, and demand response.

Sigurd Bjarghov (Student Member, IEEE) received the M.Sc. degree in electric power engineering from the Norwegian University of Science and Technology (NTNU), Trondheim, Norway, in 2017, and where he is currently pursuing the Ph.D. degree in consumer-centric market design. Since 2017, he has been with NTNU. His research interests include local electricity markets, future balancing markets, optimization, and demand response.

Venkatachalam Lakshmanan received the Ph.D. degree in electrical engineering from the Technical University of Denmark, Risø, Denmark, in 2016. He was affiliated with Electricity Markets and Energy System Planning Group, Department of Electric Power Engineering, Norwegian University of Science and Technology as a Postdoctoral Fellow from 2017 to 2019. He is currently employed as a Research Scientist with SINTEF Energy As. His research interests include power systems planning, modeling flexibility, demand response, energy storage integration, and optimization.

Ari Hentunen (Member, IEEE) received the M.Sc. (Tech.) degree from the Helsinki University of Technology, Espoo, Finland, in 2005, and the D.Sc. (Tech.) degree from Aalto University, Espoo, in 2016. He is a Research Scientist with VTT Technical Research Centre of Finland, Electrical Powertrains and Storage Team. His main interests are grid integration and operational optimization of battery storages, performance and lifetime characterization of batteries, and battery health diagnostics.

Juha Forsström received the M.Sc. degree from the Department of Technical Physics, Helsinki University of Technology (now Aalto University), in 1984. Since 1984, he has been with VTT (Technical Research Centre of Finland) carrying out research in energy systems. His interests include energy systems, modelling and quantitative decision making support.

Stig Ødegaard Ottesen received the M.Sc. degree in electrical power engineering, and the Ph.D. degree in industrial economics and technology management from the Norwegian University of Science and Technology in 1987 and 2017, respectively. He is currently working as the Head of R&D, eSmart Systems. His research interests include power systems and power markets, smart grid technologies and related business models, market design, and decision support modeling in general.

Roberto Villafafila-Robles (Member, IEEE) received the M.Sc. degree in industrial engineering, and the Ph.D. degree in electrical engineering from the School of Industrial Engineering of Barcelona, Universitat Politècnica de Catalunya (UPC), Barcelona, Spain, in 2005 and 2009, respectively. He is currently an Associate Professor with the Electrical Engineering Department of UPC at teaches the ETSEIB and EEBE. Since 2003, he has been with the Centre of Technological Innovation in Static Converters and Drives, UPC, where he is involved in technology transfer with the local industry due to research and innovation. His research interests include integration of renewable energy-storage-electrical vehicles into power systems, electricity markets, and energy and territory

Andreas Sumper (Senior Member, IEEE) was born in Villach, Austria. He received the Dipl.-Ing. degree in electrical engineering from the Graz University of Technology, Austria, in 2000, and the Ph.D. degree from the Universitat Politècnica de Catalunya, Barcelona, Spain, in 2008. From 2001 to 2002, he was a Project Manager for innovation projects in the private sector. In 2002, he joined the Center for Technological Innovation in Static Converters and Drives (CITCEA), Universitat Politècnica de Catalunya. Since 2006, he has been teaching with the Department of Electrical Engineering. He is currently a Full Professor with the Escola Superior d'Enginyeria Industrial de Barcelona, Universitat Politècnica de Catalunya. His research interests are renewable energy, digitalization of the power grid, micro- and smart grids, power system studies, and energy management.